eprints@whiterose.ac.uk
https://eprints.whiterose.ac.uk/

Nano-scratch, nanoindentation and fretting tests

of 5-80 nm ta-C films on Si(100)

B.D. Beake[1,2,*], M.I. Davies[1], T.W. Liskiewicz[3], V.M. Vishnyakov[2] and S.R. Goodes[1]

[1] Micro Materials Ltd., Willow House, Ellice Way, Yale Business Village,

Wrexham, LL13 7YL, UK, Ben@micromaterials.co.uk

[2] Dalton Research Institute, Manchester Metropolitan University,

Manchester M1 5GD, UK

[3] Institute of Engineering Thermofluids, Surfaces & Interfaces, School of Mechanical

Engineering, University of Leeds, Woodhouse Lane, Leeds, LS2 9JT, UK

* Corresponding author, email: ben@micromaterials.co.uk

Abstract

Wear and stiction forces limit the reliability of Silicon-based micro-systems when mechanical contact occurs. Ultra-thin filtered cathodic vacuum arc (FCVA) ta-C films are being considered as protective overcoats for Si-based MEMS devices. Fretting, nano-scratch and nanoindentation of different thickness (5, 20 and 80 nm) ta-C films deposited on Si(100) has been performed using spherical indenters to investigate the role of film thickness, tangential loading, contact pressure and deformation mechanism in the different contact situations. The influence of the mechanical properties and phase transformation behaviour of the silicon substrate in determining the tribological performance (critical loads, damage mechanism) of

the ta-C film coated samples has been evaluated by comparison with previously published data on uncoated Silicon. The small scale fretting wear occurs at significantly lower contact pressure than is required for plastic deformation and phase transformation in nanoindentation and nano-scratch testing. There is a clear correlation between the fretting and nano-scratch test results despite the differences in contact pressure and failure mechanism in the two tests. In both cases increasing film thickness provides more load support and protection of the Si substrate. Thinner films offer significantly less protection, failing at lower load in the scratch test and more rapidly and/or at lower load in the fretting test.

1. Introduction

Wear and stiction forces limit the reliability of Silicon-based micro-systems (e.g. MEMS) when mechanical contact occurs [1-3]. Silicon exhibits highly complex mechanical and tribological behaviour with phase transformations and lateral cracking observed in indentation and brittle fracture in a wide range of mechanical contacts [4-6]. It exhibits little or no conventional plasticity at room temperature and its deformation is dominated by phase transformation and fracture. Its nanoindentation behaviour has been extensively studied [7-12]. It has been established that a phase transformation to metallic behaviour occurs beneath the contact site and the pop-out during unloading is a consequence of phase transformation and volumetric expansion. Less well studied is its behaviour under the type of more complex loading geometries that can occur in practical tribological situations [13] so we recently investigated the behaviour of highly polished Si(100) under different contact situations, using a nanomechanical test system to perform nanoindentation, nano-scratch and 10000 cycle small scale fretting tests all with the same 4.6 μm sphero-conical diamond indenter [14-15]. Tangential loading in the nano-scratch and fretting tests promoted non-elastic yield at lower critical load. Silicon showed subtle rate sensitivity in the nano-scratch and nanoindentation tests but the wear behaviour in the fretting test was more strongly dependent on the rate of

initial loading. When the load was applied abruptly in <0.3 s, radial and lateral cracking and material removal was observed and large displacement jumps (pop-ins) were observed during the subsequent fretting test. In contrast, when the load was applied more slowly in 10 s radial cracking was not observed and there was a distinct threshold load at around 100 mN marking the transition to a more severe wear mode with extensive lateral cracking and material removal.

Several approaches are being considered including liquid lubrication [16], and solid lubrication with self-assembled monolayers [17], ALD [18, 19] and carbon films [20-23]. Particularly promising results on actual MEMS devices have been obtained for conformal deposition strategies (WS_2 by ALD [19], DLC by PECVD [20]). Tetrahedral amorphous carbon (ta-C) films deposited by FCVA have been developed for MEMS applications including capacitive sensors and protective coatings for micromachined components [21-23]. The mechanical and interfacial behaviour of the contacting silicon surfaces is modified by these thin, low surface energy films. Nanoindentation with a Berkovich indenter has shown that the films are hard (hardness of 80 nm ta-C is ~22 GPa) and elastic [24-25]. This high hardness and H/E is due to >70% sp^3 [26] but the films can be highly stressed if deposited to too great thickness [27-28]. Nano-scratch testing of ta-C films has shown that they are sufficiently thin to not show large area delamination and scratch resistance increases with H/E [24-25]. Increasing the ta-C thickness from 5 to 80 nm was found to increase the critical load for film delamination by a factor of two.

In this current study nanoindentation and nano-scratch tests have been performed on 5, 20 and 80 nm ta-C films with a 4.6 µm radius probe, and fretting with 5 and 37 µm probes to determine (i) rate sensitivity of pop-outs during unloading in nanoindentation (ii) whether the thin ta-C films influence the occurrence of large pop-ins at high load in nanoindentation (iii)

the extent of rate sensitivity in film failure in the nano-scratch test (iv) the influence of the ta-C on lateral cracking thresholds in nano-scratch testing (v) the mechanism of film failure in the fretting test and the influence of film thickness on the fretting wear. The influence of the mechanical properties and phase transformation behaviour of the silicon substrate in determining the tribological performance (critical loads, damage mechanisms) of the ta-C film coated samples has been investigated by comparison with previously published [14-15] data on uncoated Silicon acquired with the same probe and experimental conditions.

2. Experimental

Nanoindentation and nano-scratch tests were performed on ta-C films deposited on silicon wafers with a commercial ultra-low drift nanomechanical test system (NanoTest, Micro Materials Ltd.) fitted with a 4.6 μm end radius sphero-conical diamond indenter which was calibrated by nanoindentation measurements on a fused silica reference sample over a wide load range. ta-C films of 5, 20 and 80 nm thickness were deposited on Si(100) substrates by FCVA [24-25]. The substrates were ultrasonically cleaned with deionized water for 10 min, followed by drying with a static neutralizing blow off gun. The samples were placed in the deposition chamber of an industrial filtered cathodic vacuum arc system (Nanofilm Technologies Pte. Ltd.) evacuated to a base pressure lower than 1×10^{-6} torr. Prior to deposition, the silicon surface was sputtered by an argon ion beam from a dc ion beam source for 3 min to remove the native oxide. The substrate holder was in floating bias. The film thickness of the 20-80 nm films was measured by a surface profiler and the thickness of the 5 nm film was estimated from the deposition rate. The R_a surface roughness was 1.8, 2.1 and 3.1 nm for the 5, 20 and 80 nm films respectively [24]. The influence of the films on the composite film-substrate response was investigated by comparing results to those on an

uncoated highly polished 300 μm thick Si(100) wafer provided by PI-KEM (Tamworth, UK) using the same 4.6 μm sphero-conical diamond indenter.

Three repeat indentation tests to 10, 50, 100, 200, 300, 400, 500 mN peak load, loading and unloading in 20 s, with a 5 s hold at peak load were performed on the 5, 20 and 80 nm films. Further tests were performed on the 80 nm ta-C to a range of peak loads and unloading rates with a 5 s hold at peak load:- (i) Peak load = 100 mN, loading rate = 5 mN/s; unloading rate = 1-50 mN/s, 10 repeats for each unloading rate; (ii) Peak load = 200 mN, loading rate = 10 mN/s; unloading rate = 1-50 mN/s, 20 repeats for each unloading rate. In all tests a 60s hold at 90% unloading was used to correct the data for (any) thermal drift.

Nano-scratch tests to 200 mN were performed on the 80 nm ta-C film tests over a wide range of loading rates (dL/dt = 0.1-12 mN/s) and scan speeds (dx/dt = 0.1-40 μm/s) to provide critical load data over a range of dL/dx = 0.1-100 mN/μm. 1-5 repeat tests were performed for each set (11 in total) of experimental conditions. Tests were performed as multi-pass (3-scan) experiments (topography-scratch-topography) that were subsequently analysed in the NanoTest software to determine the on-load and residual depth data, following the procedure described in reference 18. Additional scratch tests were carried out on the ta-C films and uncoated Si(100) to a peak load of 300 mN with a loading rate of 12 mN/s and scanning speed 10 μm/s to investigate lateral cracking (3 repeats on Si, 5 on the ta-C films). All tests were spaced at least 50 μm apart.

The fretting tests were performed in a NanoTest Vantage system using 5 and 37 μm diamond probes whose end radii were calibrated by nanoindentation testing over a wide load range on fused silica and sapphire (0001) reference samples. The configuration for small scale fretting

includes an additional oscillating stage with a multi-layer piezo-stack to generate sample motion. The piezo movement is magnified by means of a lever arrangement to achieve larger amplitudes [29]. The fretting track length was set at 10 μm and the oscillation frequency 5 Hz. Fretting experiments of differing number of wear cycles and applied load were performed in normal laboratory conditions (~50 % RH) on the ta-C films as summarised in Table 1. The mean initial Hertzian contact pressures in the tests ranged from ~3-4 GPa at 10 mN to ~10 GPa at 200 mN using the 37 μm probe and were ~6 GPa using the 5 μm probe. Adjacent tests were spaced 100 μm apart. Tangential (friction) force data were acquired simultaneously with depth data throughout the nano-scratch and fretting tests using a lateral force transducer which was calibrated by a method of hanging masses.

Table 1 Fretting test experimental conditions

	5 nm ta-C	20 nm ta-C	80 nm ta-C
R = 37 µm, L = 1 mN		900 cycles	
R = 37 µm, L = 10 mN	300, 600, 900, 1500, 3000, 6000, 9000, 18000 cycles	1500, 3000, 6000, 9000, 18000 cycles	
R = 37 µm, L = 50 mN		300, 600, 900, 1500, 3000, 6000, 9000 cycles	1500, 3000, 6000, 9000, 18000 cycles
R = 37 µm, L = 200 mN			300, 600, 900, 1500, 3000, 6000, 9000, 18000 cycles
R = 5 µm, L = 10 mN			1500, 3000, 6000, 9000, 18000 cycles

The Electron microscopy was done utilising Zeiss Supra 40 VP (variable pressure) electron microscope. Secondary electron imaging was done by conventional (Everhart-Thornley) and In-Lens secondary electron detector. The detectors have different sensitivity to the surface charge and topography, when In-Lens detector is more sensitive to surface charging and less sensitive to topography. Surface charging can be caused by the surface enrichment with oxygen (oxidation) and this was utilised in this communication. Backscattering is strongly affected by average atomic number when heavier species, like silicon, have higher backscattering coefficient then the lighter one like carbon. When carbon film is thin, like in

this paper, part of the backscattering signal is coming from top carbon layer and part of the signal from silicon. If across the scan view the thickness of carbon varies, then more signal is coming where carbon thickness is less. The Silicon Drift Detector from EDAX was used to obtain qualitative results of film composition and thickness. The results were obtained at 5 keV electron beam in order to increase top layer sensitivity. Fully quantitative results in the situation with the variable composition and thickness films on a substrate can only be obtained in conjunction with modelling and will be published later. The line scans presented in the paper can be used for the qualitative analysis.

3. Results

3.1 Nanoindentation

Figure 1 (a) shows illustrative nanoindentation curves to 500 mN on all of the samples. Large pop-ins (extensive lateral cracking) were observed occasionally at >400 mN, as in one of the tests shown on the 80 nm ta-C, but there was no obvious dependence of the critical loads required on film thickness. Figure 1 (b) shows typical nanoindentation curves to 100 mN on the 80 nm film and uncoated Si(100). At low load the curves are elastic and virtually identical as both are due to the elastic behaviour of the Silicon. As the load increases small but clear differences are observed with pop-ins on Si at ~37 mN, at ~43 mN on the 80 nm film and an additional pop-in at higher load, more obviously on the ta-C film at ~76 mN. The pop-out during unloading occurs at higher load on the uncoated Si. Figure 1 (c) shows the variation in pop-out load after unloading from 100 or 200 mN at 1-50 mN/s together with previously reported [15] data on Si(100) acquired with the same probe and experimental conditions for comparison. Pop-ins are less clear in the 200 mN tests where loading was at 10 mN/s than in the tests to 100 mN at 5 mN/s.

8
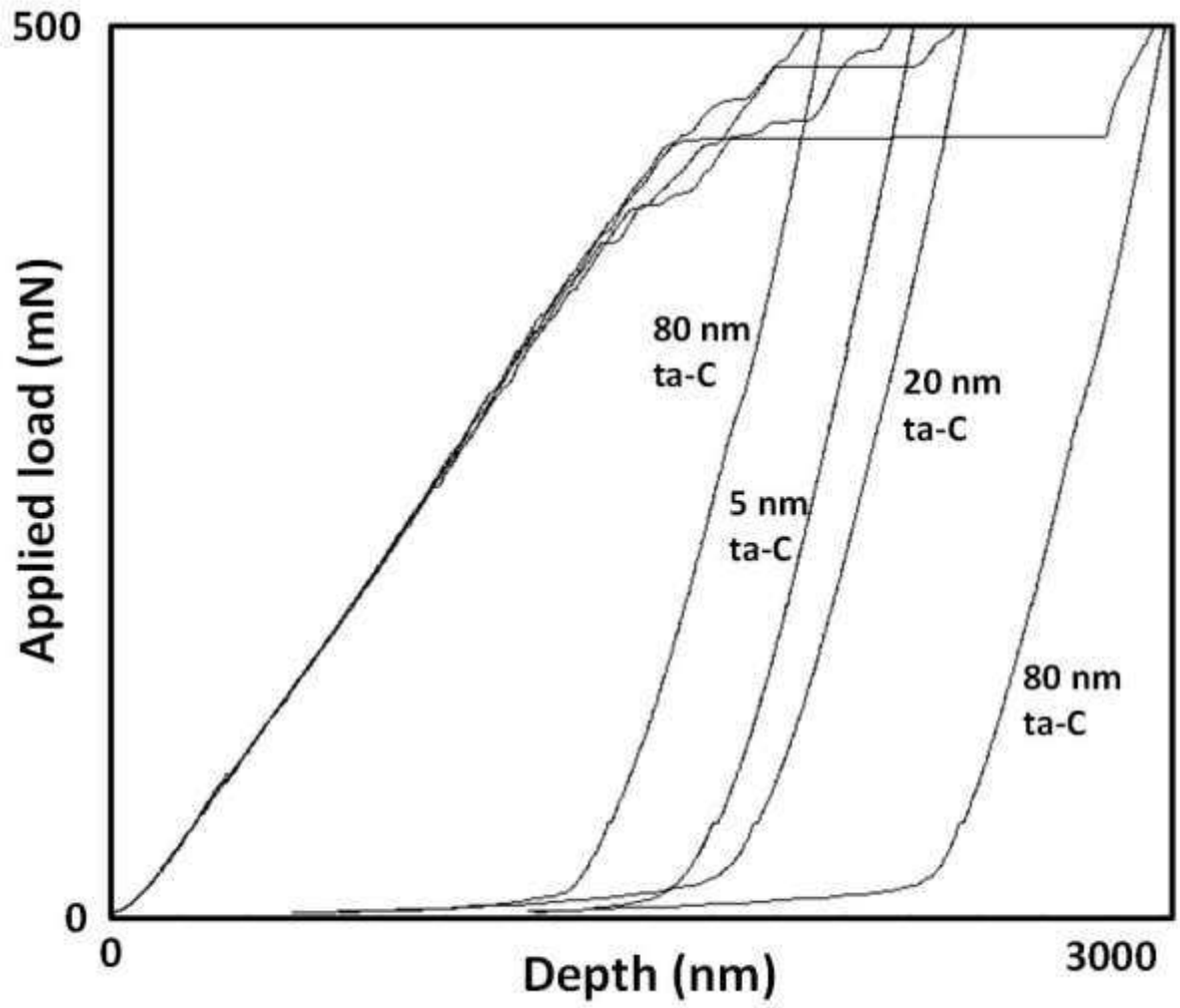
Figure 1 (a) typical nanoindentation curves to 500 mN on 5, 20 and 80 nm ta-C
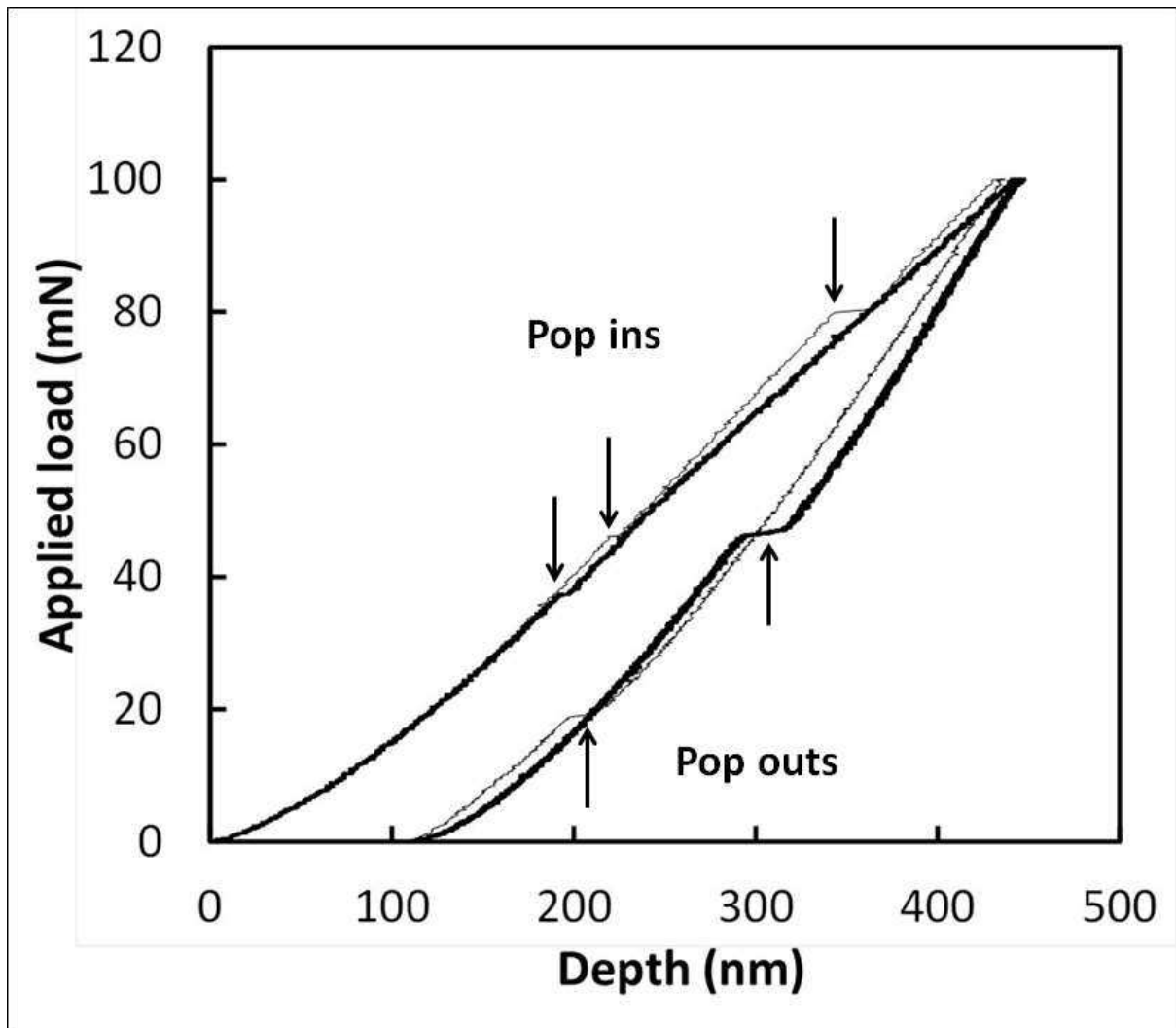
Figure 1 (b) Typical nanoindentation curves to a peak load of 100 mN on Si (thicker line) and 80 nm ta-C (thinner line). Unloading rate = 2.5 mN/s. The pop-ins during loading are marked with down arrows and the pop-outs during unloading marked with up arrows.
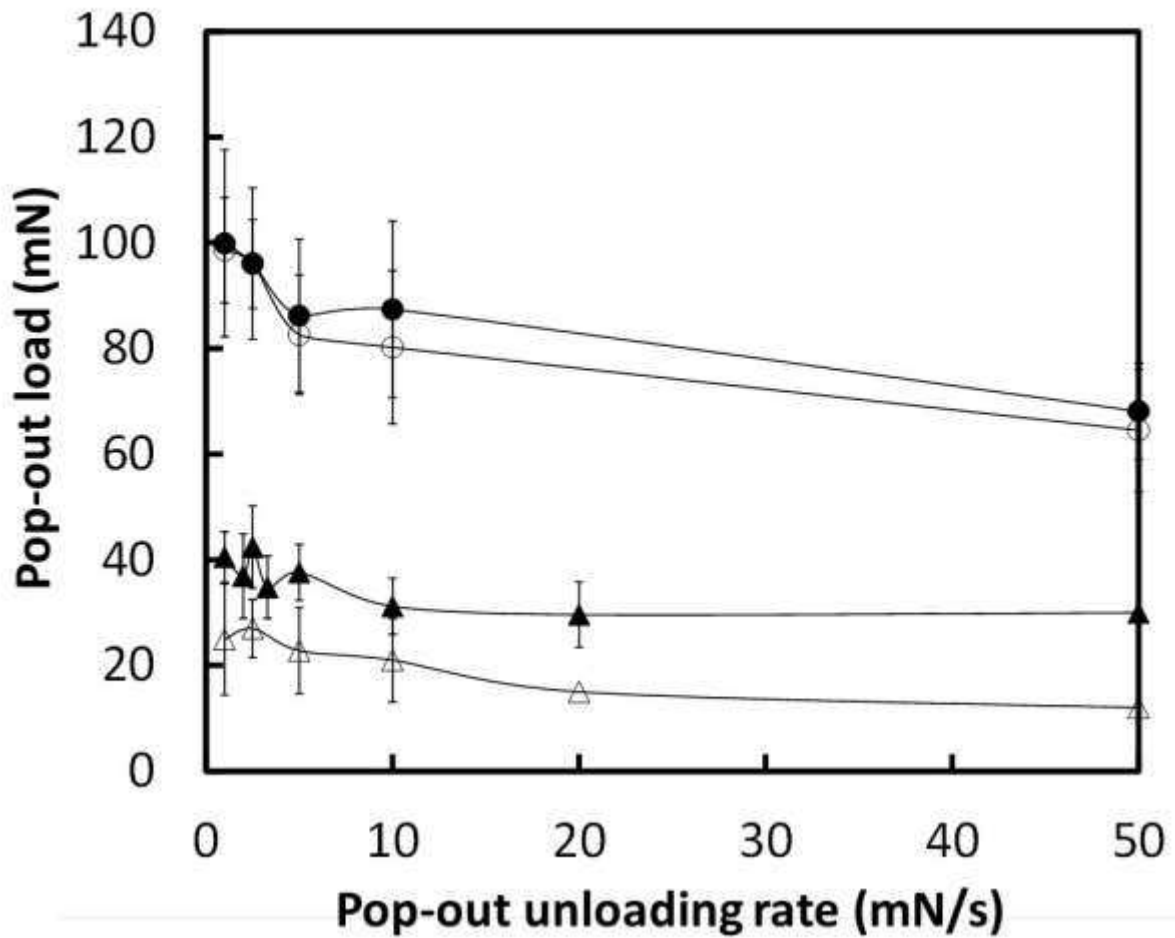
Figure 1 (c) Variation in critical load for pop-out with unloading rate on Si (filled symbols) and 80 nm ta-C (open symbols). The peak load was 200 mN for the circles and 100 mN for the triangles.

3.2 Nano-scratch

The films exhibited the expected critical load transitions as the load increased. A depth trace from a typical test is shown in figure 2 (a). The data shown has been corrected for topography, sample slope and instrument compliance following the procedure described in reference 25, allowing true depth data to be displayed under the scratch load and at minimal

scanning force (after load removal). In this example the onset of non-elastic behaviour (L_y) occurs after 136 μm (44 mN). At L_{c1} (192 μm, 71 mN) there is step in the residual depth data and total film failure occurs a depth change of just over 80 nm at L_{c2} (266 μm, 108 mN). Backscattered SEM images confirm total film failure and substrate exposure at this point (e.g. insert in figure 2 (b)).
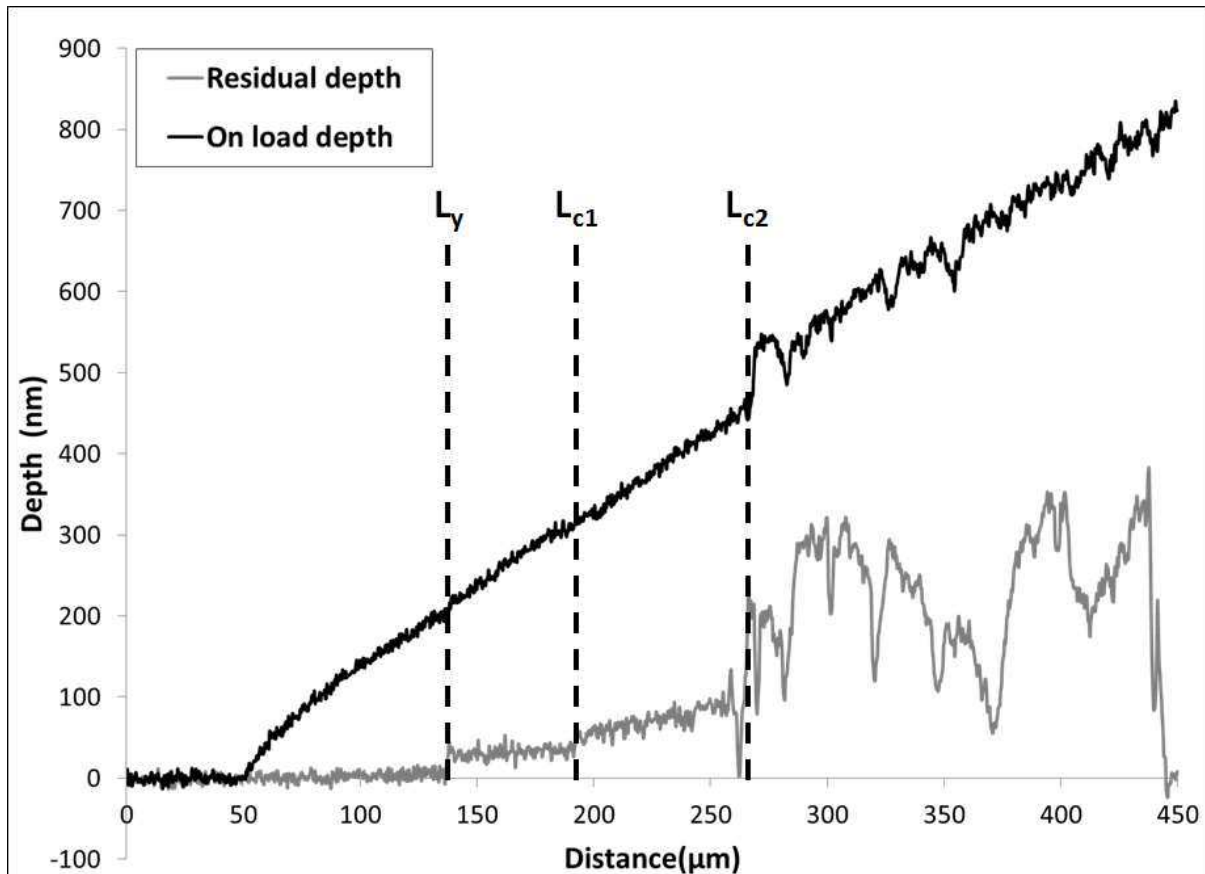
Figure 2 (a) Nano-scratch behaviour of the 80 nm ta-C film. Loading rate = 1 mN/s. Scan speed = 2 μm/s.

On the 80 nm ta-C clear film failure (L_{c2}) was observed in all the tests to 200 mN but lateral cracking (L_{c3}) was absent. Above the critical load for edge cracking, L_{c1}, but prior to the total film failure some isolated small delamination events could occasionally be seen in the scratch

12

track. SEM images (e.g. figure 2 (b)) show periodic cracking across the scratch track between L_{c1} and L_{c2}. At film failure the abrupt change in depth is very close to the film thickness.
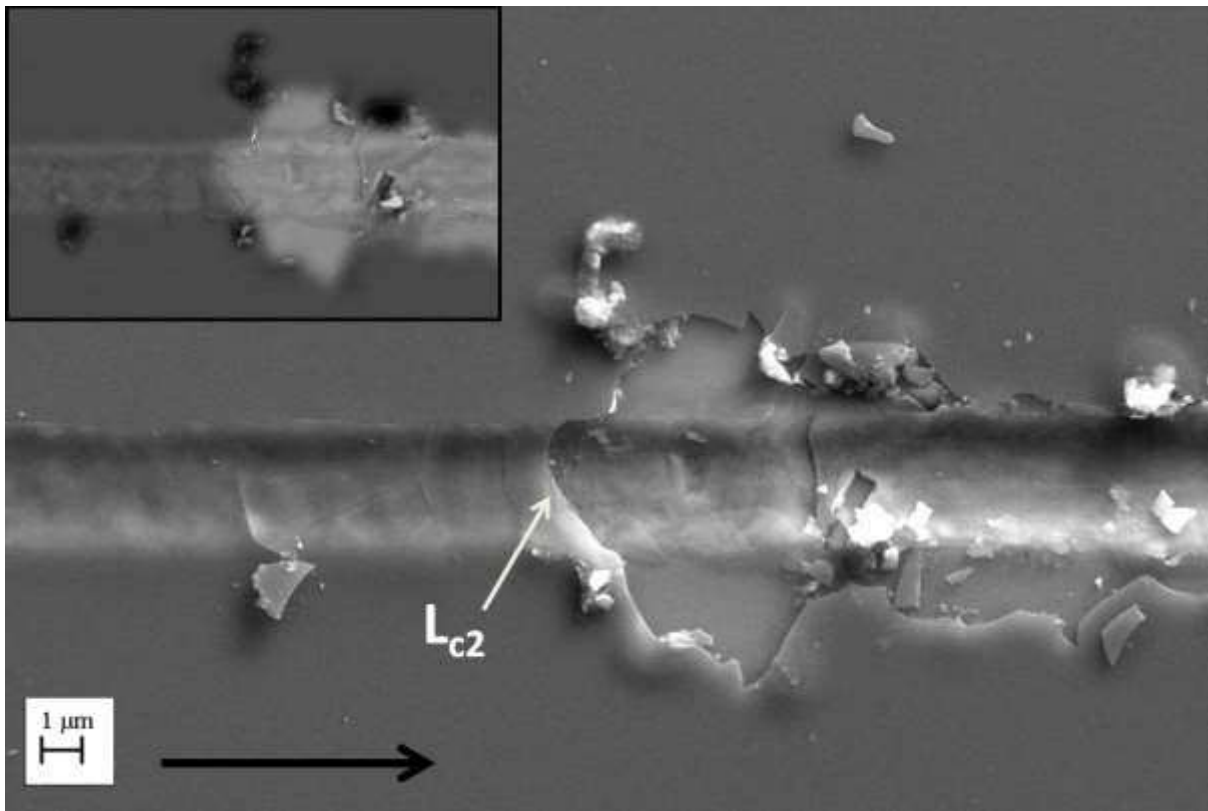
Figure 2 (b). SEM image of the scratch on the 80 nm ta-C film shown in figure 2 (a) showing L_{c2} failure preceded by cracking across the scratch track (main image = SE image, insert = back-scatttered image). The scratch direction (left to right) is shown by an arrow on the SE image.
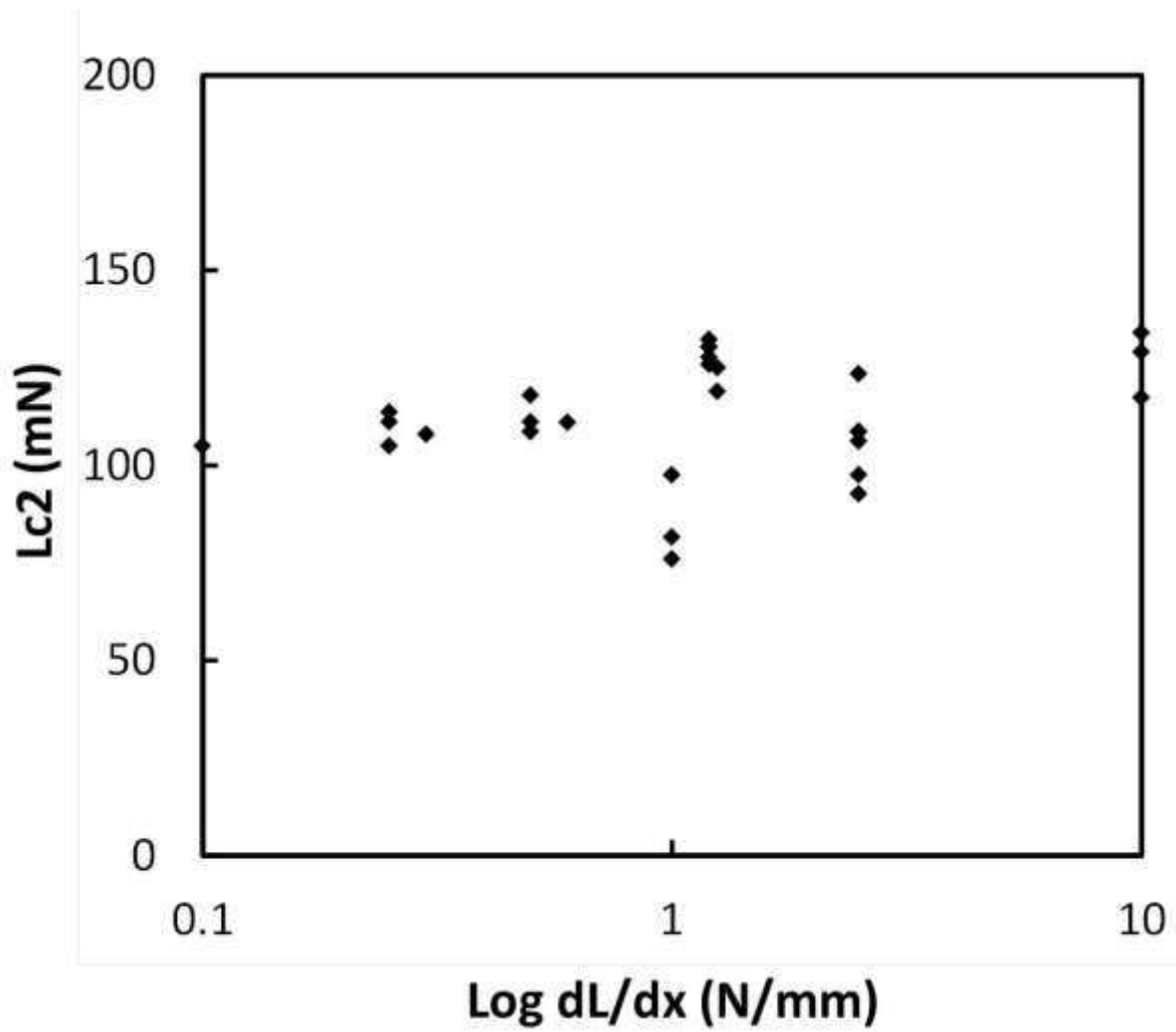
Figure 2 (c) Variation in the critical load for film failure (L_{c2}) in the nano-scratch test with dL/dx for the 80 nm ta-C film.

Table 2 Critical load for lateral cracking in nano-scratch tests

	Si	5 nm ta-C	20 nm ta-C	80 nm ta-C
L_{c3} (mN)	130 ± 10	152 ± 35	163 ± 45	276 ± 20

Figure 2 (c) shows the variation in L_{c2} vs. dL/dx for the 80 nm ta-C film. Friction coefficients were ~0.09 at yield, ~ 0.14-0.15 at L_{c2} film failure and ~0.21-0.24 at the onset of lateral

14

cracking. The variation in the critical load for lateral cracking with film thickness is shown in Table 2. The critical load for the L_{c3} failure increased dramatically on the 80 nm ta-C and the lateral cracking was less pronounced. For the uncoated, 5 and 20 nm ta-C film sample the scratch track is more jagged after L_{c3} due to the more extensive lateral cracking (figure 3).
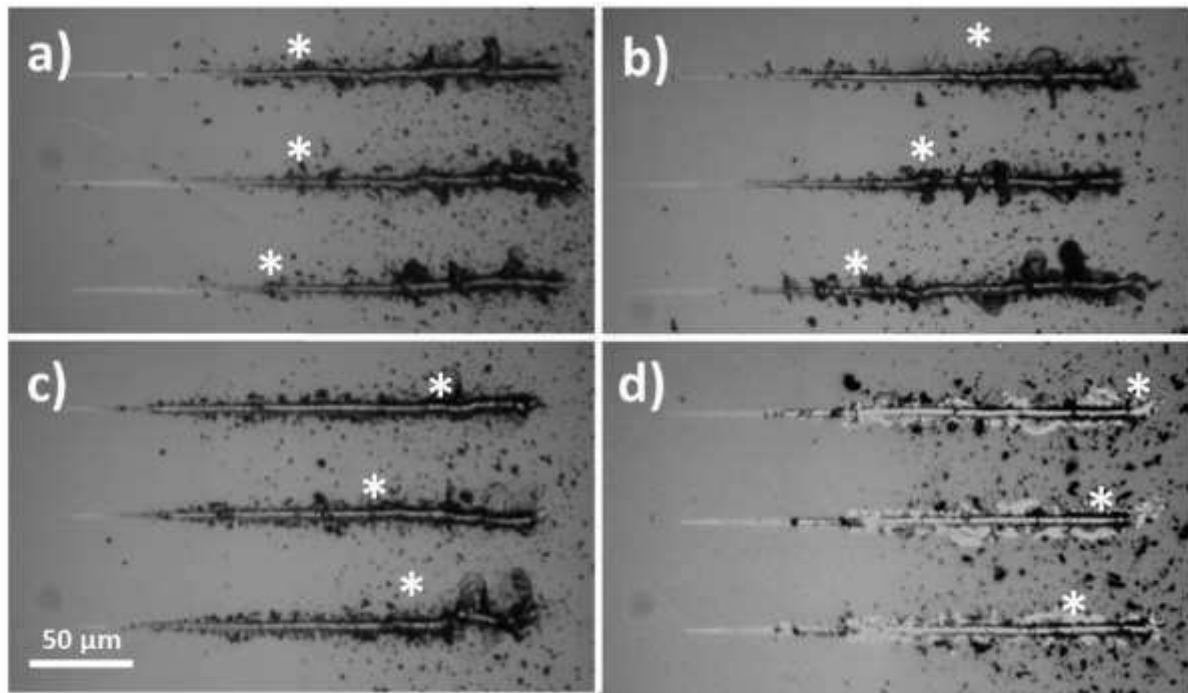
Figure 3. Optical micrographs of nano-scratches to 300 mN on (a) uncoated Si, (b) 5 nm ta-C, (c) 20 nm ta-C and (d) 80 nm ta-C films. The onset of lateral cracking (L_{c3} failure) is marked by an asterisk.

3.3 Fretting and SEM/EDX analysis of fretting scars

The on-load probe depth did not show abrupt steps during the fretting tests, more typically showing an initial slight decrease before a transition point after which it increased progressively through the test. The point marking the onset of the increase in depth was accompanied by a gradual increase in the friction. Friction coefficients at film failure were

15

typically (0.10 ± 0.01). In the fretting of the 20 nm ta-C film at 50 mN the friction and on-load depth signals show a transition occurring at >1500 cycles. SEM/EDX analysis of the fretting tests stopped after 1500 and 3000 cycles was performed to investigate the behaviour in more detail (figure 4).
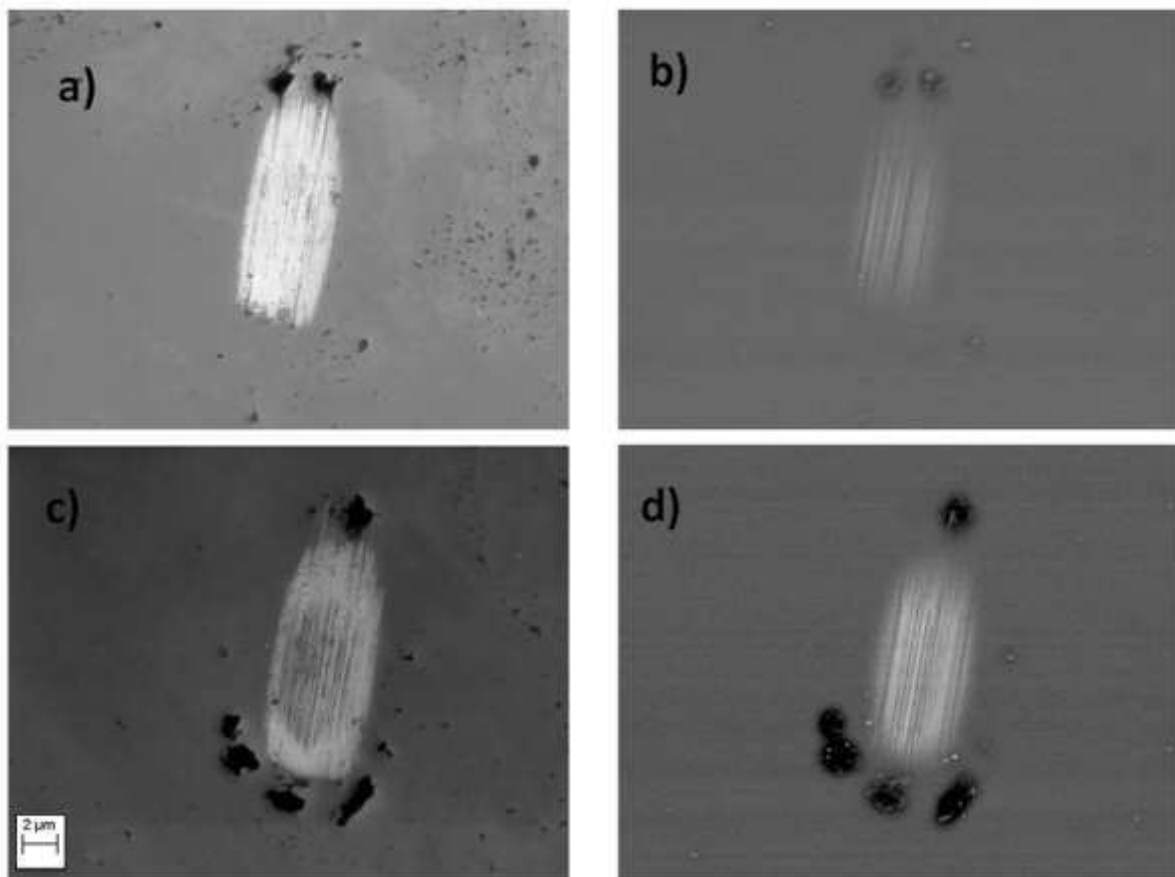
Figure 4. SEM imaging of wear scars after fretting the 20 nm ta-C film at 50 mN for 1500 cycles (a = SE image, b = back-scatttered image) and 3000 cycles (c = SE image, d = back-scatttered image).
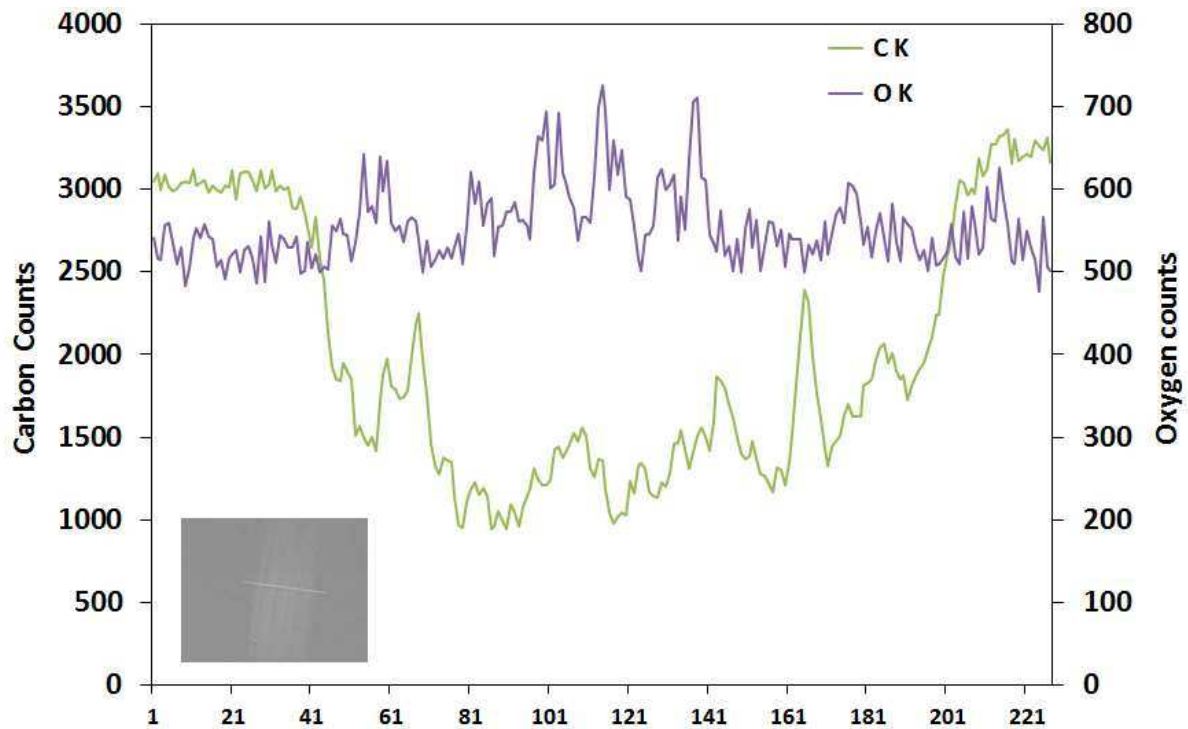
Figure 5. EDX line profile across the wear scar corresponding to the 1500 cycle test shown in figure 4 (a-b).

EDX line profiles across the fretting wear scar of the 1500 cycle test revealed thinning of the 20 nm film and oxygen incorporation in the worn region (figure 5). The worn scar of the 3000 cycle test showed more oxygen incorporation in the track and in the debris particles together with some exposed Silicon due to removal of the film and the C signal dropped to zero. 300 cycle tests also showed reduction in coating thickness and oxygen incorporation. Similar behaviour was observed on the 5 nm film at 10 mN with oxygen incorporation and film thinning within 1500 cycles and complete removal of the film from the wear scar region in the 3000 cycle test. EDX analysis of short duration fretting wear scars on the 80 nm ta-C film did not show the same oxygen incorporation as on the thinner films. For the 80 nm film, at 200 mN with the 37 μm probe, the total film failure occurs between 3000 and 6000 cycles. Comparison of tests at 50 mN shows the 20 nm film was worn through after a smaller

17

number of cycles than the 80 nm film, and at 10 mN similarly the 5 nm film is worn away more rapidly than the 20 nm film. Wear scars from 18000 cycle tests on the 80 nm ta-C showed a reduction in track length at 200 mN compared to 50 mN.

4. Discussion

The presence of the ta-C film affects the phase transformation behaviour of the Si by providing load support, reducing the effective load reaching the substrate and spreading the deformation out over a wider area. Critical loads for pop-ins and pop-outs are modified by the presence of the ta-C overlayer. While their exact positions change, the rate dependence of them is virtually identical with and without the ta-C (e.g. see figure 1(iii)) confirming that they are due to transitions in the underlying Si rather than the film. It is interesting to compare and contrast this behaviour with that observed for thicker films. Haq and co-workers used SEM, focussed ion beam microscopy (FIB) and cross-sectional transmission electron microscopy (XTEM) techniques to investigate the deformation occurring in indentation contacts with a 5 µm probe for Si coated with 1.6 µm RF a-C:H [30], 600 nm RF a-C:H [31] and a 30 GPa 170 nm FCVA ta-C [26]. For the 1.6 µm a-C:H they found that at 100 mN the coating showed a reduction in thickness of ~4.5 % but there was no deformation at the interface or in the substrate and phase transformation was suppressed. At 100 mN on the 600 nm a-C:H film they observed 4.4% compressive strain in the coating, some bending at the interface with some slight delamination and some plastic deformation accompanied phase transformation. From the presence of slip without transformed material at 50 mN they suggested therefore that plastic deformation in the Si rather than phase transformation or any coating cracking was responsible for the first pop-in. For the 170 nm ta-C film they observed plastic deformation in the Si for indentation loads as low as 10 mN, with the first observable

pop-ins at 12-18 mN and phase transformation and cracking at higher loads. Even though the indentation depth at 10 mN was over 50 % of the film thickness XTEM showed no evidence for plastic compression of the coating, only some bending at the interface. As with the thicker film, the first critical load at ~15 mN was assigned to slip in the Si and the second at ~24 mN to phase transformation. Although the 170 nm ta-C film was harder (30 GPa) than the 80 nm ta-C, Haq et al reported a penetration depth at 10 mN of ~100 nm which could suggest that the radius of the tip was actually considerably less than the nominal 5 µm and/or it has developed some asperity damage at the tip. This would provide an explanation of why the critical loads in that study were observed at much smaller loads than in all of the reported tests on Si(100) with 4.2-5.0 µm indenters [7,8,15,32]. In the current work with a 4.6 µm end radius probe the on-load indentation depth was only ~75 nm for all the ta-C films and we did not see any critical loads until ~44 mN. Although it is conceivable that the first pop-in in the 80 nm film/Si system is a result of plastic deformation phase transformation is at least as likely, as indentations to 50 mN on the 80 nm ta-C show an elbow event (phase transformation) in unloading at ~10 mN. For uncoated Si, the first pop-in − which XTEM shows is due to phase transformation - occurs around 40 mN with this 4.6 µm probe, consistent with reported values of 28 mN with a 4.2 µm probe [7,8] and 37 mN with a 5 µm probe [32]. On uncoated Si phase transformation (elbowing) during unloading was observed on unloading from 55-65 mN.

Nevertheless, some localised slip may occur at low load in the 80 nm ta-C system; evidence for the influence of the film in initially retarding phase transformation but promoting slip in the substrate is provided by the presence of in the much larger pop-out that occurs on the film at around 70-85 mN than on the uncoated Si where a smaller pop-out occurs at ~80-95 mN. It seems reasonable to assume that this is phase transformation. In unloading from 100 mN (figure 1(c)) characteristic pop-outs are observed for both Si and the 80 nm film/Si system.

Since the rate dependence is virtually identical with and without the film, it is clear that these relate to the same process in the silicon, with the presence of the ta-C film retarding the pop-outs, as has been observed for thicker systems and in our own work with a sharper Berkovich indenter where the mean pop-out load unloading from a peak load of 20 mN at 0.5 mN/s decreased from 4.7 mN on the uncoated Si to 4.0 mN and 3.3 mN for 20 nm and 80 nm ta-C respectively [24].

The influence of film thickness and indenter radius on the critical loads for yield, edge cracking and total film failure in the nano-scratch test have been extensively studied previously. With a 3.1 µm end radius probe a contact pressure of about 12 GPa was required for yield on the 5, 20 and 80 nm films. Hertzian analysis of contact pressure at failure using the 4.6 µm probe gives a contact pressure of (15 ± 1) GPa for the 80 nm film at L_{c2}, which is close to the value of 14.5 GPa previously determined with the 3.1 µm probe. Chang and Zhang have reported that in Berkovich indentation of uncoated Si (100) the critical load for pop-in is around 14 GPa, close to a theoretical value of 14.3 GPa for the transition from Si-I to Si-II under spherical indentations [11]. They therefore interpreted the inelastic deformation as being solely due to phase transformation. After the pop-in the contact pressure dropped to ~12 GPa, i.e. the hardness of silicon. Although tangential loading promotes yield (as described in [15] for uncoated Si(100)) the contact pressures in indentation and nano-scratch of Si or coated Si are not that different as the friction at yield is low.

Here we were also interested in the lateral cracking (L_{c3} failure) that occurs on Si at higher load and whether the ta-C films could protect the substrate or not. The nano-scratch test data show that tangential loading promotes the formation of large lateral cracks on all the ta-C film samples at much lower load than in nanoindentation as was recently observed for uncoated Si(100) [15]. The occurrence of large pop-ins at high load when Silicon is indented with spherical indenters has been shown to be highly stochastic in nature, with Oliver and co-

workers reporting a threshold load of (350 ± 100) mN with a 4.3 µm probe and larger pop-ins (>1 µm) more likely at >500 mN [33]. In the limited number of high load nanoindentation tests performed the thin hard ta-C films showed no significant protection against lateral cracking, which occurred only occasionally, irrespective of the ta-C film thickness. However, in the nano-scratch test the tangential loading promoted dramatic film failure at much lower load (e.g. ~115 mN for 80 nm ta-C; see figure 2) with extensive lateral cracking occurring below 300 mN. Marked differences emerged for the 80 nm film where the critical load for this L_{c3} failure increased dramatically and the lateral cracking was less pronounced. These thin films do not show any of the large-area delamination outside the scratch track commonly observed on failure of thicker hard and elastic (high H/E) coatings [34]. It appears that when the film fails in the scratch track, the intact ta-C film outside the scratch track is capable of maintaining a measure of load support and providing some protection.

Although, as expected for a brittle material, Silicon has been shown to be very rate sensitive in rapid (<0.3 s) loading [14] or at high sliding speeds [35], in our previous study of the rate dependence of its behaviour in the nano-scratch test [15] we noted only a small dependence of the critical load on dL/dx, which was consistent with similarly small kinetic effects on the phase transformation events observed in nanoindentation testing with the same probe. Nano-scratch tests on the 80 nm ta-C film on Si have been performed over a much wider range of dL/dx in the current study revealing minimal rate dependence, with the critical load for film failure being (113 ± 15) mN over a 100-fold variation in dL/dx from 0.1-100 mN/µm. This very small rate-sensitivity in the scratch response is consistent with previous studies of a-C:H and a-C:H/Si films on glass which showed no obvious rate sensitivity over a 20-fold range of dL/dx from 0.05-1 mN/µm [36]. The increase in friction force with load follows closely the behaviour observed on uncoated Si. In both cases this is due to increasing ploughing contribution to the friction force as the severity of the contact increases. Similar behaviour

21

was observed by Sundararajan and Bhushan in AFM-nanoscratching, where friction coefficients on 3.5-20 nm ultra-thin carbon films were initially 0.04-0.06, which was the same as Si(100) tested under the same conditions, increasing to ~0.1 at the critical load [37,38]. Liu et al reported that graphitic layers at the surface (~3 nm) were responsible for lower friction coefficients of ~0.09 on ta-C than other a-C:H films [39]. Tangential loading with friction can promote yield, with the magnitude of the decrease depending on the friction as shown by Zok and Miserez [40]. Blees and co-workers reported that the critical load in scratching sol-gel coatings on polypropylene decreased by an order of magnitude when the friction increased from 0.5 to 3 [41]. However, the friction coefficient is only 0.07 at yield on Si so the effect was rather small, with critical loads for yield (first pop-in) being (40 ± 5) mN in indentation and (37 ± 5) mN in nano-scratch. Wu and co-workers noted a reduction in the critical load for phase transformation in nano-scratching compared to nanoindentation [42]. As the friction coefficient at yield of the ta-C films is only 0.09, it is unsurprising that there was little difference in the critical load for yield in the nano-scratch test being generally no lower than in nanoindentation.

In the fretting test deformation proceeds by a fatigue mechanism with a gradual wearing away of the film, as shown by the EDX profiles across scars, and the absence of any abrupt changes in depth or friction. Li and Bhushan reported that fatigue wear and fatigue-induced delamination occur in reciprocating sliding of ta-C films depending on film thickness [43]. Wilson and Sullivan reported a similar process in nano-fretting of 10-150 nm a-C films deposited on Si by closed field unbalanced magnetron sputter ion plating (CFUBMSIP) [44-46]. This fatigue wear process is in marked contrast to the behaviour in the nano-scratch test where the contact pressure is greater and distinct critical loads are observed, with abrupt increases in probe depth and friction. Appreciable substrate deformation and bending at the film-substrate interface is necessary before the thin films fail. The probe depths under load at

failure are significantly lower in the fretting test due to lower substrate deformation and consequently the friction force at failure is lower in the fretting test due to a smaller contribution from ploughing. A similar friction coefficient (0.09-0.12) was found by Qian and co-workers in low-cycle nano-fretting of NiTi shape memory alloy with a 50 μm diamond when the contact pressure was sufficiently low that ploughing was minimized [47]. Hertzian analysis can be used to estimate the contact pressure at the start of the reciprocation in the fretting tests assuming initially elastic contact. For the 37 µm probe this gives ~3-4 GPa at 10 mN, ~8 GPa at 50 mN and 9-11 GPa at 200 mN. For the 5 µm probe this gives ~6 GPa. The on-load probe depth data typically show a small reduction during the first wear cycles which may be due to blistering, delamination, phase transformation and oxygen incorporation. Hillocks have been shown to form at contact pressures > 1 GPa in nano-fretting tests in an AFM on Si(100) [48] and volume uplift due to the phase transformation of the underlying Si may be occurring here. Hard carbon films are known to suffer from poor adhesion and delamination-induced blistering, and in repetitive spherical nanoindentation of 500 nm DLC films on Si(100) blistering and delamination of the film resulted in a reduction of indentation depth with loading cycles when a spherical indenter was used [49].

Li and Bhushan proposed a mechanism for fatigue failure of 3.5-20 nm ta-C films in reciprocating sliding with 3 mm sapphire sliders. In this mechanism wear fatigue cracks form in the coating and on thinner (3.5, 5 nm ta-C) propagate to the interface resulting in delamination but for 20 nm do not reach the interface. We have previously noted that this mechanism does not take into account substrate deformation and interface bending and therefore is not directly applicable to the behaviour in the nano-scratch test where appreciable elastic and plastic substrate deformation occurs and failure does not occur until the probe depth is greater than the film thickness. In the small scale fretting test the mechanism of film

failure is closer to that proposed by Li and Bhushan although some substrate deformation does occur.

Analysis of the SEM images of fretting wear scars revealed distinctive gross-slip type of damage with scratches generated during sliding present within the wear scar area. The damage mechanics of ta-C films seems to be progressive wear by debris generation and debris aggregation outside the contact area. Wang and Kato observed transitions from no-wear to a wear particle regime in low cycle pin on disk testing of CN_x coatings in an SEM over the contact pressure range 5-18 GPa [50]. At low load initially only "feather-like" particles were produced and with increasing wear cycles a transition to "plate-like" particles was found [50]. In macro-scale reciprocating wear of Si [43,51] or ta-C films [52] a significant running in period of high friction has been reported. This has been interpreted as adhesive wear resulting from the low real area of contact and high local stresses. Fretting wear particles were generated and as the test progressed a transition to flake morphology and deep grooves in the wear track due to abrasive wear was observed. In the nano-scale tests the running-in period was much shorter. As a result of using 37 µm radius probe rather than 5 µm, no cracking or coating delamination, as observed in the case of nano-scratch test, has been observed around fretting wear scars even under maximum load of 200 mN. The geometry of the wear scars correlated with the loads applied and wider wear tracks were observed as a result of higher contact pressures and larger Hertzian contact radius. The reduction in wear track length with increased load from 50 to 200 mN on the 80 nm ta-C is consistent with other studies of small-scale fretting [53]. EDX analysis confirmed coatings perforation for longer tests with EDX line scans showing higher oxygen content and lower carbon counts due to thinning of coatings. Low cycle tests showed coating thinning and corresponding oxide formation even after short 300-cycle experiments. Oxygen incorporation in the thinner films may limit their durability. Recent molecular dynamics simulations have

indicated oxidation as a possible mechanism in the sliding wear of ta-C films [54]. With the 5 μm probe the 80 nm ta-C film wears readily at a much lower load of 10 mN. The maximum von Mises stress is well into the substrate (at a depth ~260 nm) and the applied load below that required for Si phase transformation. Fretting damage may be initiated by micro-slip in the substrate, as has been shown in low load indentations of 170 nm ta-C films. Phase transformation is expected to play a key role since De-kun and co-workers have shown that ion implantation of Si(111) significantly improved its wear resistance in a reciprocating wear test [51], presumably as the amorphous near-surface layer formed did not undergo phase transformations in contact in the same way.

5. Conclusions

The presence of the ta-C film affects the phase transformation behaviour of the Si by providing load support, reducing the effective load reaching the substrate and spreading the deformation out over a wider area. Critical loads for pop-ins and pop-outs are modified by the presence of the ta-C overlayer. While their exact positions change, the rate dependence of them is virtually identical with and without the ta-C confirming that they are due to transitions in the underlying Si rather than the film. The nano-scratch test data show that tangential loading promotes the formation of large lateral cracks on all the ta-C film samples at much lower load than in nanoindentation. Increasing the ta-C film thickness to 80 nm significantly increased the critical load for this lateral cracking. Small scale fretting wear occurs at significantly lower contact pressure than is required for plastic deformation and phase transformation in nanoindentation and nano-scratch testing. There is a clear correlation between the fretting and nano-scratch test results despite the differences in contact pressure and failure mechanism in the two tests. In both cases increasing film thickness provides more load support and protection of the Si substrate. Thinner films offer significantly less

protection, failing at lower load in the scratch test and more rapidly and/or at lower load in the fretting test.

6. Acknowledgements

7. References

1. J.A. Williams and H.R. Le, Tribology and MEMS, J. Phys. D: Appl. Phys. 39 (2006) R201-R214.

2. D.M. Tanner, W.M. Miller, W.P. Eaton, L.W. Irwin, K.A. Peterson, M.T. Dugger et al, The effect of frequency on the lifetime of a surface micromachined microengine driving a load, 1998 IEEE International Reliability Physics Symposium Proceedings, March 30 – April 2, 1998, pp. 26-35.

3. I.S.Y. Ku, T. Reddyhoff, A.S. Holmes, H.A. Spikes, Wear of silicon surfaces in MEMS, Wear 271 (2011) 1050-1058.

4. R.F. Cook, Strength and sharp contact fracture of silicon. J. Mater. Sci. 41 (2006) 841.

5. S. Bhowmick, H. Cha, Y.-G. Jung, B.R. Lawn, Fatigue and debris generation at indentation-induced cracks in silicon, Acta. Mater. 57 (2009) 582-589.

6. V. Domnich, Y. Gogotsi, Phase transformations in silicon under contact loading, Rev. Adv. Mater. Sci. 3 (2002) 1-36.

7. J.E. Bradby, J.S. Williams, J. Wong-Leung, M.V. Swain, P. Munroe, Mechanical deformation of crystalline silicon during nanoindentation, Mat. Res. Soc. Symp. Proc. 649 (2001) Q8.10.

8. J.E. Bradby, J.S. Williams, J. Wong-Leung, M.V. Swain, P. Munroe, Mechanical deformation in silicon by microindentation, J. Mater. Res. 16 (2001) 1500-1507.

9. T. Juliano, Y. Gogotsi, V. Domnich, Effect of indentation unloading conditions on phase transformation induced events in silicon, J. Mater. Res. 18 (2003) 1192-1201.

10. T. Juliano, V. Domnich, Y. Gogotsi, Examining pressure-induced phase transformations in silicon by spherical indentation and raman spectroscopy: A statistical study, J. Mater. Res. 19 (2004) 3099-3108.

11. L. Chang, L.C. Zhang, Deformation mechanisms at pop-out in monocrystalline silicon under nanoindentation, Acta. Mater. 57 (2009) 2148-2153.

12. L. Chang, L.C. Zhang, Mechanical behaviour characterisation of silicon and effect of loading rate on pop-in: A nanoindentation study under ultra-low loads, Mater. Sci. Eng. A 506 (2009) 125-129.

13. A. Matthews, S. Franklin, K. Holmberg, Tribological coatings: contact mechanisms and selection, J. Phys. D: Appl Phys. 40 (2007) 5463-5475.

14. B.D. Beake, T.W. Liskiewicz, N.J. Pickford, J.F. Smith, Accelerated nano-fretting testing of Si(100), Tribol. Int. 46 (2012) 114-118.

15. B.D. Beake, T.W. Liskiewicz and J.F. Smith, Deformation of Si(100) in spherical contacts – comparison of nano-fretting and nano-scratch tests with nanoindentation, Surf. Coat. Technol. 206 (2011) 1921-1926.

16. I.S.Y. Ku, T. Reddyhoff, R. Wayte, J.H. Choo, A. S. Holmes, H.A. Spikes, Lubrication of microelectromechanical devices using liquids of different viscosities, J. Tribol. 134 (2012) 012002-1.

17. R. Maboudian, W.R. Ashhurst, C. Carraro, Self-assembled monolayers as anti-stiction coatings for MEMS: characterisation and recent developments, Sensors Actuators, 82 (2000) 219-223.

18. C. Nistorica, J.-F. Liu, I. Gory, G.D. Skidmore, F.M. Mantiziba, B.E. Gnade et al, J. Vac. Sci. Technol. A 23 (2005) 836.

19. T.W. Scharf, S.V. Prasad, M.T. Dugger, P.G. Kotula, R.S. Goeke and R.K. Grubbs, Growth, structure, and tribological behaviour of atomic layer-deposited tungsten disulphide solid lubricant coatings with applications to MEMS, Acta Mater. 54 (2006) 4731-4743.

20. S.A. Smallwood, K.C. Eapen, S.T. Patton and J.S. Zabinski, Performance results of MEMS coated with a conformal DLC, Wear 260 (2006) 1179-1189.

21. N. Akita, Y. Konishi, S. Ogura, M. Imamura, Y.H. Hu and X. Shi, Comparison of deposition methods for ultra thin DLC overcoat film for MR head, Diamond Relat. Mater. 10 (2001) 1017-1023.

22. C.Y. Chan, K.H. Lai, M.K. Fung, W.K. Wong, I. Bello, R.F. Huang, C.S. Lee, S.T. Lee and S.P. Wong, Deposition and properties of tetrahedral amorphous carbon films prepared on magnetic disks, J. Vac. Sci. Technol. A 19 (2001) 1606.

23. Shi, B.K. Tay, H.S. Tan, L. Zhong, Y.Q. Tu, S.R.P. Silva and W.I. Milne, Properties of carbon ion deposited tetrahedral amorphous carbon films as a function of ion energy, J. Appl. Phys. 79 (1996) 7234-7240.

24. B.D. Beake, S.P. Lau, Nanotribological and nanomechanical properties of 5-80 nm tetrahedral amorphous carbon films on silicon, Diam. Relat. Mater. 14 (2005) 1535-1542.

25. B.D. Beake, S.R. Goodes, B. Shi, Nanomechanical and nanotribological testing of ultra-thin carbon-based and MoST films for increased MEMS durability, J. Phys. D: Appl. Phys. 42 (2009) 065301.

26. A.J. Haq, P.R. Munroe, M. Hoffman, P.J. Martin, A. Bendavid, Nanoindentation-induced deformation behaviour of tetrahedral amorphous carbon coating deposited by flitered cathodic vacuum arc, Diam. Relat. Mater. 19 (2010) 1423-1430.

27. D. Sheeja, B.K. Tay, K.W. Leong and C.H. Lee, Effect of film thickness on the stress and adhesion of diamond-like carbon coatings, Diam. Relat. Mater. 11 (2002) 1643-1647.

28. D. Sheeja, B.K. Tay, S.P. Lau, K.W. Leong and C.H. Lee, An empirical relation for critical load of DLC coatings prepared on silicon substrates, Int. J. Mod. Phys. B 16 (2002) 958-962.

29. T.W. Liskiewicz, B.D. Beake, J. F. Smith, In situ accelerated micro-wear − a new technique to fill the measurement gap, Surf. Coat. Technol. 205 (2010 1455-1459.

30. A.J. Haq, P.R. Munroe, M. Hoffman, P.J. Martin, A. Bendavid, Nanoindentation-induced deformation behaviour of diamond-like carbon coatings on silicon substrates, Thin Solid Films 515 (2006) 1000-1004.

31. A.J. Haq, P.R. Munroe, M. Hoffman, P.J. Martin, A. Bendavid, Effect of coating thickness on the deformation behaviour of diamond-like carbon-silicon system, Thin Solid Films 518 (2010) 2021-2028.

32. E.R. Weppelmann, J.S. Field, M.V. Swain, J. Mater. Sci. 30 (1995) 2455.

33. D.J. Oliver, B.R. Lawn, R.F Cook, M.G. Reitsma, J.E. Bradbury, J.S. Williams et al, Giant pop-ins in nanoindented silicon and germanium caused by lateral cracking, J. Mater. Res. 23 (2008) 297-301.

34. B.D. Beake, V.M. Vishnyakov, R. Valizadeh, J.S. Colligon, Influence of mechanical properties on the nanoscratch behaviour of hard nanocomposite TiN/Si_3N_4 coatings on Si, J. Phys. D: Appl. Phys. 39 (2006) 1392-1397.

35. X. Li, J. Lu, B. Liu, S. Yang, Tribological behaviour and phase transformation of single-crystal silicon in air, Tribol. Int. 41 (2008) 189-194.

36. B.D. Beake, A.A. Ogwu, T. Wagner, Influence of experimental factors and the film thickness on the measured critical load in the nano-scratch test, Mater. Sci. Eng. A 423 (2006) 70-73.

37. S. Sundararajan, B. Bhushan, Development of a continuous microscratch technique in an atomic force microscope and its application to study scratch resistance of ultrathin hard amorphous carbon coatings, J. Mater. Res. 16 (2001) 437-445.

38. S. Sundararajan, B. Bhushan, Micro/nanotribology of ultra-thin hard amorphous carbon coatings using atomic force microscopy, Wear 225-229 (1999) 678-689.

39. D. Liu, G. Benstetter, E. Lodermeier, X. Chen, J. Ding, Y. Liu, J. Zhang, T. Ma, Surface and structural properties of ultrathin diamond-like carbon coatings, Diam. Relat. Mater. 12 (2003) 1594-1600.

40. F.W Zok, A. Miserez, Property maps for abrasion resistance of materials, Acta Mater. 55 (2007) 6365-6371.

41. M.H. Blees, G.B. Winkelman, A.R. Balkenende, J.M.J. den Toonder, The effect of friction on scratch adhesion testing: application to a sol-gel coating on polypropylene, Thin Solid Films 359 (2000) 1-13.

42. Y.Q. Wu, H. Huang, J. Zou, L.C. Zhang, J.M. Dell, Nanoscratch-induced phase transformation of monocrystalline Si, Scripta Mater. 63 (2010) 847-850.

43. X. Li and B. Bhushan, Micro/nanomechanical and tribological characterization of ultrathin amorphous carbon coatings, J. Mater. Res. 14 (1999) 2328-2337.

44. G.M. Wilson, J.F. Smith, J.L. Sullivan, A DOE nano-tribological study of thin amorphous carbon based films, Tribol. Int. 42 (2009) 220.

45. G.M. Wilson, J.F. Smith, J.L. Sullivan, A nanotribological study of thin amorphous C and Cr doped amorphous C coatings, Wear 265 (2008) 1633.

46. G.M. Wilson, J.L. Sullivan, An investigation into the effect of film thickness on nanowear with amorphous carbon-based coatings, Wear (2009) 1039.

47. L. Qian, Z. Zhou, Q. Sun and W. Yan, Nanofretting behaviours of NiTi shape memory alloy, Wear 263 (2007) 501-507.

48. J. Yu, L. Qian, B. Yu, Z. Zhou, Nanofretting behaviour of monocrystalline Silicon (100) against SiO_2 microsphere in vacuum, Tribol. Lett. 34 (2009) 31-40.

49. N.H. Faisal, R. Ahmed, Y.Q. Fu, Y.O. Elakwah, M. Alhoshan, Influence of indenter shape on DLC film failure during multiple load cycle nanoindentation, Mater. Sci. Technol. 2012 in press.

50. D.F. Wang, K. Kato, In situ examination of wear particle generation in carbon nitride coatings by repeated sliding contact against a spherical diamond, Wear 253 (2002) 519-526.

51. Z. De-kun, G. Shi-rong, W. Qing-liang, Research on the fretting wear behaviour of silicon wafers before and after carbon ions implantation, Tribol. Int. 42 (2009) 1399-1404.

52. E. Zdravecka, V.M. Tiainen, Y.T. Konttinen, L. Franta, M. Vojs, M. Matron, M. Ondac, J. Tkacova, Relationship between the fretting wear behaviour and mechanical properties of thin carbon films, Vacuum 86 (2012) 675-680.

53. B. Raeymaekers, S. Helm, R. Brunner, E.B. Fanslau, F.E. Talke, Investigation of fretting wear at the dimple/gimbal interface in a hard drive suspension, Wear 268 (2010) 1347-1353.

54. G. Moras, L. Pastewka, P. Gumbsch and M. Moseler, Formation and oxidation of linear carbon chains and their role in the wear of carbon materials, Tribol. Lett. 44 (2011) 35-365.